Controller Structure Design Using Power System Stabilizers in Multimachine Power System

Joe H. Chow†, Haoxing Ren†, Shaopeng Wang†, Glauco N. Taranto‡, Nelson Martins§

† ECSE Department, Rensselaer Polytechnic Institute, Troy, NY 12180–3590, USA

‡ Electrical Engineering Department, COPPE/UFRJ, Rio de Janeiro, RJ 21945–970, Brazil.

§ CEPEL, Rio de Janeiro, RJ 21944–970, Brazil.

Abstract: This paper investigates two controller structures suitable for damping power swings in multimachine power systems. The structures consist of a decentralized controller design involving two power system stabilizers and a controller design using a remote signal and only one power system stabilizer. We provide an analysis of the decentralized control design, which motivates the input signal synthesis using the remote signal. The impact of communication delays in using the remote signal is investigated. The design is illustrated using a 5-machine equivalent of the South/Southeast Brazilian system, which has an open-loop unstable intearea mode and cannot be stabilized using only one conventional power system stabilizer and local measurements as input signals.

Keywords: Small-Signal Stability, Power System Stabilizers, Robust Control, Decentralized Control, Linear Matrix Inequalities, Remote Signals, Communication Delay

I. Introduction

In an interconnected power system, oscillatory modes can be local, affecting only a few machines, or global, affecting machines over a wide area. Stability and damping control designs involving many machines have to impose a hierarchical structure in order to be effective, reliable, and robust [1]. A control designer must weigh the merits of various controller structures such as centralized and decentralized designs, as well as the use of any remote signals.

In this paper, we investigate two controller structures for the design of power system stabilizers (PSS) in a small equivalent Brazilian system. The controller designs include a decentralized controller structure of two PSS's using only local signals, and a single PSS design using an input signal synthesized from a remote speed signal. Discussions on a centralized structure design of a two-input, two-output controller can be found in [2] and will not be repeated here.

The test system is a modified 7-bus, 5-machine equivalent model of the South/Southeast Brazilian system first presented in [3] and depicted in Figure 1. The complete system data can be obtained from [3]. This system is selected because it cannot be stabilized with a single conventional PSS. However, it can be stabilized by using two PSSs [3], [2]. In the decentralized controller structure using two PSS's, we compare the applicability of a classical design approach using the root-locus technique and of a linear matrix inequality (LMI) design approach. Then we provide a "zero-locus" analysis to explain how the application of one PSS aids the second PSS in stabilizing the unstable interarea mode.

In the second controller structure, we investigate the use of a remote signal to stabilize the system using only one PSS. A remote speed measurement is combined with a local speed signal using a zero-locus analysis to synthesize an appropriate input signal to the PSS. Because using a remote signal incurs time delays, two different schemes in synthesizing the PSS input signal are investigated. In addition, the robustness of using the remote signal in enhancing the damping of the swing modes is examined.

The paper is organized as follows. Section II provides a discussion of the 5-machine Brazilian system. Section III contains the decentralized controller de-

signs. Section IV investigates the alternative control structure using a remote signal and the robustness of the design.

II. Test System

The modal analysis of the small Brazilian test system indicates that there are two interarea modes. Mode 1 is due to the Southeast (SE) equivalent system oscillating against the Itaipu generator, while Mode 2 is due to the South system (represented by Santiago, Segredo and Areia) oscillating against the Southeast system together with the Itaipu generator. The system also has two local modes of oscillations within the South system: Mode 3 consisting of Areia and Segredo oscillating against Santiago, and Mode 4 consisting of Areia oscillating against Segredo.

Table I presents five operating scenarios, obtained from the same transmission network configuration, where the values of the reactances X_{5-6} and X_{6-7} (connecting Buses 5-6 and Buses 6-7, respectively) are varied [3]. The generator and load levels are the same for all 5 scenarios. Table I also shows the frequencies and the damping ratios of Modes 1 and 2. In all operating scenarios, Mode 1 is open-loop unstable. The local modes (Mode 3 and Mode 4) have damping ratios of about 20% and oscillation frequencies of about 1.46 Hz.

TABLE I
Open-loop Operating Conditions

Case #	X_{5-6} pu	X_{6-7} pu	Mode 1		Mode 2	
			f(Hz)	ζ(%)	f(Hz)	ζ(%)
1	0.39	0.57	0.86	-11.9	0.94	3.8
2	0.50	0.57	0.86	-12.1	0.92	3.5
3	0.80	0.57	0.85	-12.7	0.88	2.8
4	0.39	0.63	0.84	-13.7	0.93	4.0
5	0.39	0.70	0.80	-16.6	0.93	4.2

Of the five operating scenarios, we choose Case 3 as the nominal design conditioon. In addition, we investigate the control design using only the Segredo and Itaipu machines. The linearized system model is described by the two-input, two-output (TITO) state-space model

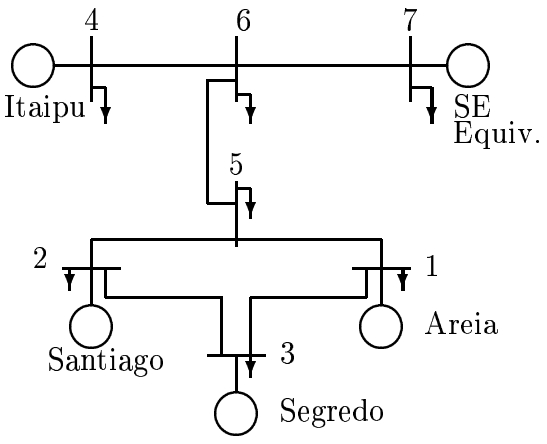

Fig. 1. Study System Configuration

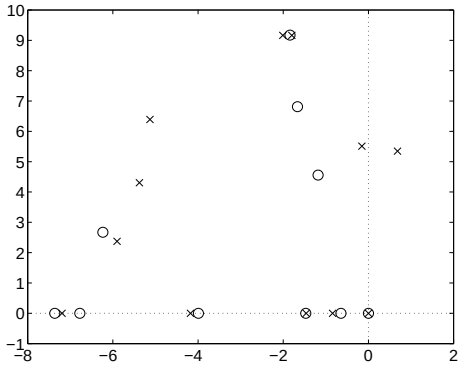

Fig. 2. Pole-Zero Plot of 2-input, 2-output System

$$\dot{x} = Ax + Bu \quad (1a)$$
$$y = Cx \quad (1b)$$
$$y = [y_{\text{Segredo}}\ y_{\text{Itaipu}}]^T \quad (1c)$$
$$u = [u_{\text{Segredo}}\ u_{\text{Itaipu}}]^T \quad (1d)$$
$$B = [B_1\ B_2] \quad (1e)$$
$$C = [C_1^T\ C_2^T]^T \quad (1f)$$

where the control signal u is the input to the Segredo and Itaipu AVR's and the measurements y are the machine rotor speeds. Figure 2 shows the multivariable pole-zero locations for the 2×2 transfer function. Note that the system is unstable with an interarea mode in the RHP (right half-plane), which is Mode 1 in Table I. However, all the zeros are in the LHP (left half-plane), allowing stabilization by applying conventional PSS's at Segredo and Itaipu.

As a comparison, we decompose the TITO system (1) into four transfer functions and compute the poles and zeros of each transfer function individually as single-input, single-output (SISO) subsystems. Figure 3(a) is the pole-zero plot of the transfer function from the Segredo input to the Segredo machine speed, which shows a RHP zero very close to the unstable pole. As a result, stability cannot be achieved by applying a conventional PSS to the Segredo machine only. Similarly, Figure 3(d) is the pole-zero plot of the transfer function from the Itaipu input to the Itaipu machine speed, which shows a RHP zero close to the $j\omega$ axis. This system still cannot be stabilized with a conventional PSS applied to the Itaipu machine only. Figures 3(b) and 3(c) show the pole-zero plots of the off-diagonal transfer function terms, namely, from the Itaipu input to the Segredo speed and from the Segredo input to the Itaipu speed. These plots show that the RHP zero is still present in these two transfer functions, and thus these transfer functions individually cannot be stabi-

lized using conventional PSSs.

Most recently, several power equipment manufacturers are marketing dual-input PSS's, which use the machine speed and electrical output power to synthesize an accelerating power variable P_{acc} [4]. One of the advantages of a dual-input PSS is that it reduces the interaction of the PSS with the excitation system mode and thus allows a higher gain to be used for improved damping. When the synthesized accelerating power variables of Segredo and Itaipu are used as the output, the main features of the pole-zero plots of the 2×2 transfer function and the individual SISO transfer functions are similar to those shown in Figures 2 and 3, and hence, the plots are omitted here. Thus using the synthesized accelerating power variable still would not allow the stabilization of the system using only a single PSS.

III. Decentralized Control Design

In this section we describe the procedures used for designing the decentralized PSS controllers. We first overview the design methods and present the design results. Then we provide an analysis to explain the mechanism allowing two decentralized PSS's to stabilize the system.

A. Classical Design

In the classical design, a double-lead compensator is applied individually to each of the Segredo and Itaipu generators' excitation systems. Each compensator is designed individually with the second compensator loop remaining open, and with the objective of providing maximum damping benefits to Modes 1 and 2 for all 5 operating conditions. Note that this is an uncoordinated design and that neither compensator can achieve stability by itself due to the presence of the RHP zeros in the open-loop transfer function of both compensators. Stability is achieved however, when both compensators are applied simultaneously. The designed compensators, including a washout stage, have the following transfer functions:

Segredo PSS

$$\text{PSS}_3(s) = 30 \times \frac{3s}{1+3s} \times \frac{(1+0.3s)(1+0.1s)}{(1+0.02s)(1+0.008s)} \quad (2)$$

Itaipu PSS

$$\text{PSS}_4(s) = 60 \times \frac{3s}{1+3s} \times \frac{(1+0.3s)(1+0.3s)}{(1+0.03s)(1+0.03s)} \quad (3)$$

The combination of these two PSS's provides satisfactorily damping to Mode 1 ranging from 7.2% to 10.6% (Table II) for all 5 operating conditions. Modes 2 has at least 50% damping. However, as common in the classical design, the PSS's interact with the machine dynamics and excitation systems to produce a lightly

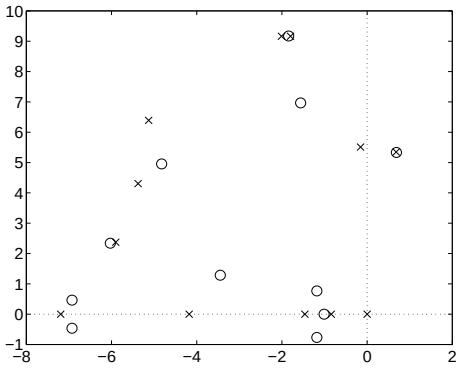

(a) System(u_{Segredo},y_{Segredo})

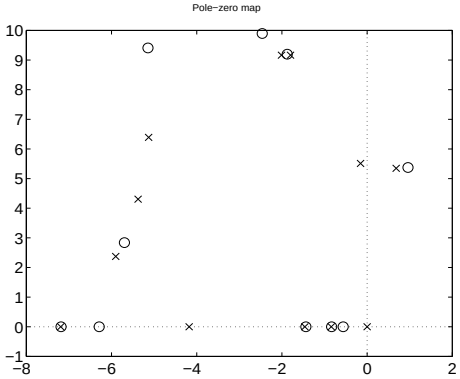

(b) System(u_{Itaipu},y_{Segredo})

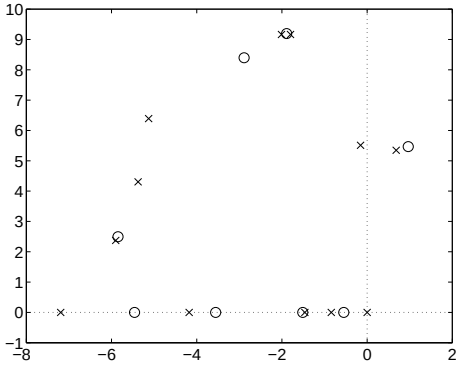

(c) System(u_{Segredo},y_{Itaipu})

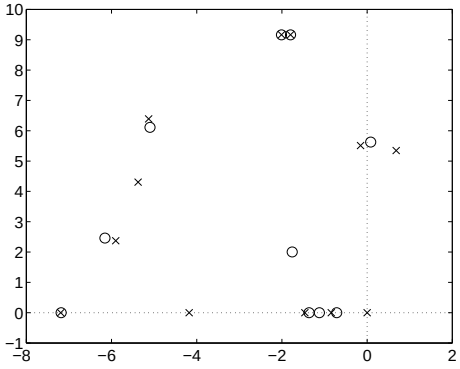

(d) System(u_{Itaipu},y_{Itaipu})

Fig. 3. Pole-Zero Plot of SISO Systems

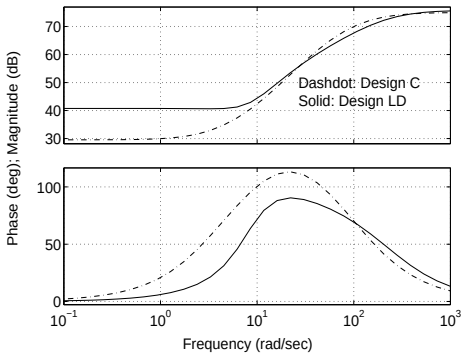

Fig. 4. Frequency Response for PSS_3, Designs C and LD

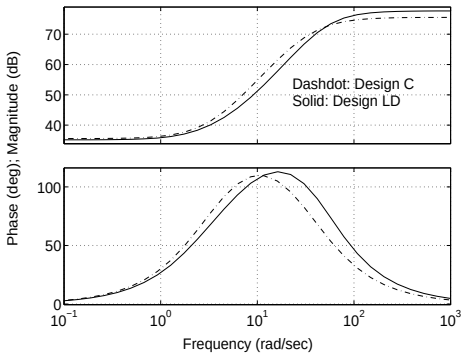

Fig. 5. Frequency Response for PSS_4, Designs C and LD

damped control mode (mode x in Table II). This classical design will be referred to as Design C. The frequency responses of these PSS's without the washout stages are shown in Figures 4 and 5.

B. LMI Design

The Linear Matrix Inequality approach presented in [8], [9] is used to design a low-order decentralized controller. In an earlier paper [8], the technique was used to design a PSS to stabilize a single-machine infinite-bus system at 5 operating scenarios. Here we are extending the results to a two-PSS design.

It is well-known that the LMI approach can solve robust control design problems with constraints such as regional pole-placement [10] through a convex optimization algorithm [11]. However, the controller obtained is of full order, that is, the same size as the design model including weighting functions. When the design problem is formulated for a low-order controller, the resulting optimization is non-convex [12]. To circumvent the non-convexity, the low-order controller LMI approach in [8] uses coprime factorization. The coprime factors allow the control design to be formulated as an approximate pole-placement problem of minimizing the H_∞ norm of a stable transfer function. The minimization can be extended to include more than one operating condition. The stability of the closed-loop system can be guaranteed by imposing a positive realness condition. This LMI approach can readily handle decentralized control by simply enforcing the gains in the off-diagonal entries of the controller to be zero in the convex optimization.

The decentralized controller obtained by adjusting the weights from the LMI design is

Segredo PSS

$$\mathrm{PSS}_3(s) = 6155 \times \frac{3s}{1+3s} \times \frac{s^2+11.3s+67}{(s+16.5)(s+230)} \quad (4)$$

Itaipu PSS

$$\mathrm{PSS}_4(s) = 7677 \times \frac{3s}{1+3s} \times \frac{(s+2.5)(s+8.2)}{s^2+94.4s+2759} \quad (5)$$

Although not having only real poles and zeros as in conventional PSS, these PSS's are phase-lead compensators. The decentralized LMI controller is denoted as Design LD. Note that an iterative LMI algorithm is used in [13] to design the decentralized PSS's. However, the non-iterative method used here and in [8] is more efficient.

Table II shows that Design LD achieves better damping than Design C for all 5 operating conditions. In particular, the control mode is well damped. The frequency responses of these two controllers are shown in Figures 4 and 5. Note that although the frequency responses of Design C and LD are quite similar, their effects on the closed-loop system poles are quite different.

C. Further Discussion on the Decentralized Design

To explain how the decentralized controllers stabilize the test system, we first close one loop of the TITO system using the Segredo machine PSS (2). The pole-zero loci plot of the Itaipu loop is obtained by varying the PSS gain of (2) from 0 to 7000 (see Figure 6). As the gain increases , Mode 2 (A) moves toward left, pulling the RHP zero (B) to the LHP between Modes 1 (A) and 2 (C). When this RHP zero moves into the LHP, we can readily design a controller to stablize the test system.

Similarly, if we close the loop on the Itaipu machine using the PSS (3), the resulting pole-zero loci plot of the Segredo loop is obtained by varying the PSS gain from 0 to 7000 as shown in Figure 7. Note that the RHP zero (D) is also pulled into the LHP when the gain increases. Thus a stablizing PSS for Segredo can be readily designed.

TABLE II

Closed-Loop System Damping Ratio (%)

Case	Design C		Design LD		Design R			Design RD		
#	Mode 1	Mode x	Mode 1	Mode 2	Mode 1	Mode 2	Mode 3	Mode 1	Mode 2	Mode 3
1	10.6	9.5	15.5	14.2	13.8	9.08	10.7	5.24	4.83	4.96
2	10.0	9.7	14.7	14.2	13.5	9.26	10.8	4.67	5.11	4.69
3	8.8	9.9	13.0	14.1	11.5	11.4	10.6	4.85	5.43	4.97
4	9.3	9.8	13.4	14.2	11.7	7.19	10.3	4.38	4.17	4.06
5	7.2	10.4	10.2	14.2	13.3	6.15	10.1	3.63	3.25	3.49

mode x – mode due to PSS interaction with excitation system.

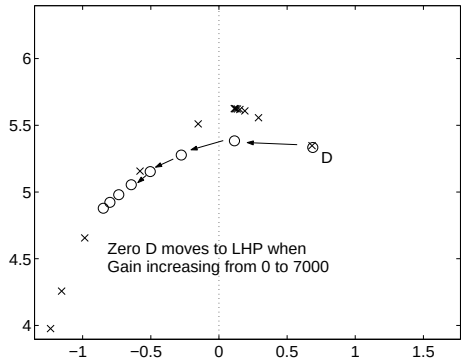

Fig. 6. Itaipu Pole-zero Plot with Segredo Loop Closed

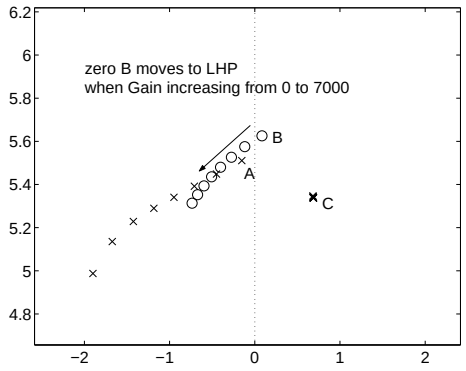

Fig. 7. Segredo Pole-zero Plot with Itaipu Loop Closed

IV. Alternative Structure using Remote Signal

In this section, we investigate an alternative controller structure that would allow the stabilization of the system with a single PSS. This strategy will be useful in enhancing the security of the system if the Segredo PSS from the decentralized controller design is not available due to outage. Because the actuators are fixed by their locations, the solution becomes a selection of alternative feedback signals. Controller input-signal designs had been investigated in [5] for SVC and in [6] for TCSC. Here we pursue a similar design strategy by synthesizing a signal whose transfer function will have more desirable zeros.

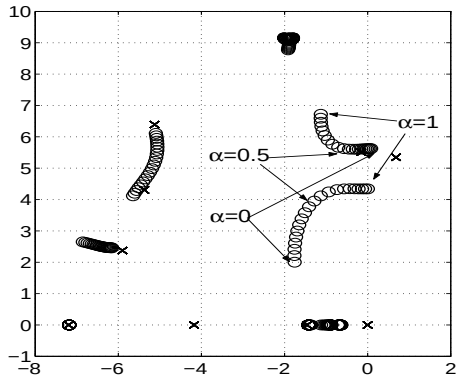

Fig. 8. Zero loci for $0 \leq \alpha \leq 1$

Based on the coherency concept [7], we propose to add the Segredo speed variable to the Itaipu speed variable with a weighting factor α to create a signal that is rich in the unstable mode (Mode 1) and yet has desirable sensitivities to add damping to Mode 2. The resulting system is

$$\dot{x} = Ax + B_2 u_{\text{Itaipu}} \tag{6a}$$

$$\overline{y}_{\text{Itaipu}} = [C_2 + \alpha C_1]x = y_{\text{Itaipu}} + \alpha y_{\text{Segredo}} \tag{6b}$$

To determine an optimal value of α, we plot the zeros of the system for values of α ranging from 0 to 1 as shown in Figure 8. Note that for this single-input, single-output system, Figure 8 traces out the zero loci, showing the RHP zero at $\alpha = 0$ moving into the LHP. On the other hand, a zero at $\alpha = 0$ in the LHP eventually moves into the RHP. To achieve a good design, we need the two zeros to be in the LHP with roughly the same real part. As a result, we set $\alpha = 0.5$. Figure 9 shows the open-loop pole-zero locations of this system, which has no RHP zeros.

For this SISO system, we use a conventional double-lead-lag compensator structure for the controller. Here we use the LMI [8] to design the compensator. To achieve the desired damping, we need to optimize the design for each of the 5 operating conditions. For example, for Case 3, the compensator, including a washout stage, has the transfer function

$$K_\alpha(s) = 204 \times \frac{3s}{3s+1} \times \frac{(s+98.8)(s+0.2)}{s^2+33.27s+812.2} \tag{7}$$

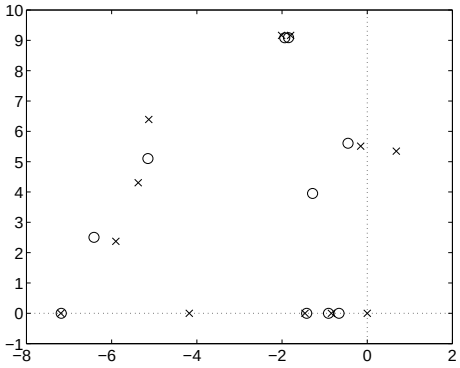

Fig. 9. Pole-Zero Plot of SISO System (u_{Itaipu},$y_{\text{Itaipu}} + \alpha y_{\text{Segredo}}$)

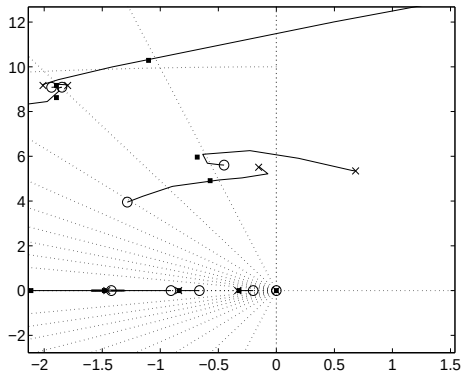

Fig. 10. Root-Locus Plot of Closed-Loop System

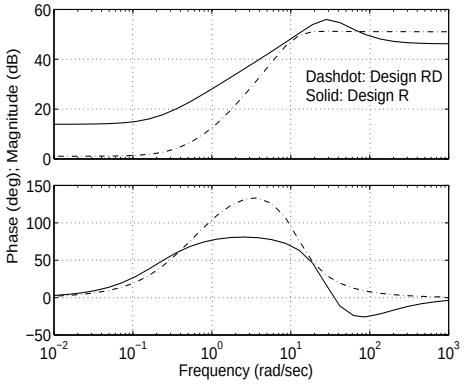

Fig. 11. Controller Frequency Response, Design R and RD

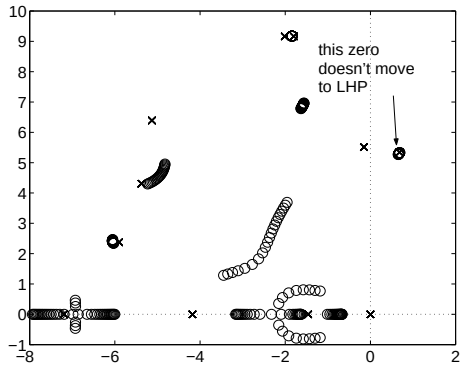

Fig. 12. Zero loci for $0 \leq \beta \leq 1$

Figure 10 is the root-locus plot of the system. This controller is denoted as Design R. Table II shows the damping of the swing modes of the feedback system for all 5 operating conditions, each using a different controller. Note that controllers are able to provide damping to both Modes 1 and 2, although the damping of Mode 3 has been reduced somewhat. The minimum damping is 6.15% for Mode 2. The frequency response of this controller without the washout stage is shown in Figure 11.

It is not unexpected that the control design with the remote signal is not as robust as the decentralized design. To implement this control scheme with 5 different controllers, it is required that the controller also monitors the system operating condition.

Although we can move the RHP zero to the LHP using the Itaipu controller, we cannot do so using the Segredo controller. The system model for the Segredo controller is

$$\dot{x} = Ax + B_1 u_{\text{Segredo}} \tag{8a}$$

$$\overline{y}_{\text{Segredo}} = [C_1 + \beta C_2]x = y_{\text{Segredo}} + \beta y_{\text{Itaipu}} \tag{8b}$$

Figure 12 shows the zero loci when β changes form 0 to 1. The RHP zero moves only slightly and remains in the RHP. The reason is that the Segredo AVR input u_{Segredo} is not as effective as the Itaipu AVR input u_{Itaipu} in controlling Mode 1.

When a remote signal is used for control, a proper design should take into account the potential delay in processing and receiving the remote signal. We now investigate the suitability of these two schemes to deal with the delay T.

In the first scheme, we simply add the delayed remote Segredo signal y_{Segredo} to the local signal y_{Itaipu} to form the synthesized signal $\overline{y}_{\text{Itaipu}}$ as in (6b). A representation of this scheme is shown in Figure 13. Note that the delay is modeled by a first-order Padé approximation [14].

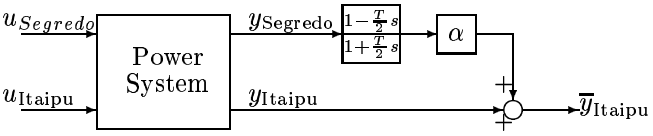

Fig. 13. Synthesized Signal with Delayed Remote Signal

Figure 14 shows the zero loci of this system as α and T change. For $T = 0.1$ sec., the zero-locus branch originating from the RHP zero does not move far away from the $j\omega$-axis. When $T \geq 0.2$ sec., that zero-locus branch does not move into the LHP at all, making it not stabilizable by a conventional PSS.

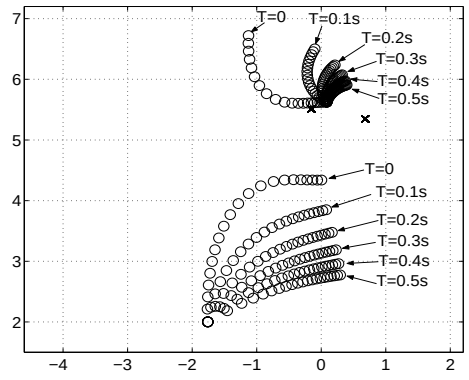

Fig. 14. Zero Loci with Various Delays

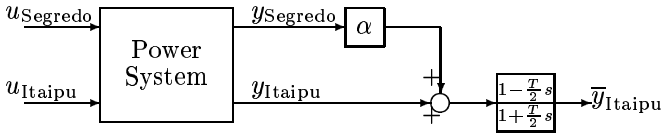

Fig. 15. Synthesized Signal with Common Delay in Remote and Local Signals

In the second scheme, we add to y_{Itaipu} the same delay as y_{Segredo}. Thus the synthesized signal can be modeled as shown in Figure 15, where both signals have the same delay, represented again by a first-order Padé approximation. The zero-locus plot of this system is identical to the one shown in Figure 8 and is independent of the delay. Comparing Figures 8 and 9, it seems that the synthesized signal scheme in Figure 14 would result in an easier design problem, because the RHP zero can be moved further into the LHP.

For the scheme in Figure 15, we propose to design a second-order PSS. With the delay, we anticipate that a larger amount of phase lead will be required. We perform the control design using the LMI method, assuming $T = 0.1$ sec. (about 5-6 cycles depending on the system frequency), which is probably a conservative estimate. Again, each of the 5 operating conditions requires a separate control design. For Case 3, the controller transfer function is

$$K_{\text{delay}}(s) = 358 \times \frac{3s(s+0.3844)(s+1.144)}{(3s+1)(s^2+15s+139.1)} \qquad (9)$$

Figure 16 shows the root-locus plot of the Case 3 system. Note that Mode 3 tends to move more rapidly toward the RHP, due to the effect of the RHP zero from the Padé approximation.

This design will be referred to as Design RD. Table II shows the damping of the swing modes of the feedback systems for all 5 operating conditions, having a minimum of 3.25% damping. Figure 11 shows that the maximum phase lead of this controller is almost 50 degrees larger than that of Design R. Although the damping is low, the controller is still useful as a backup

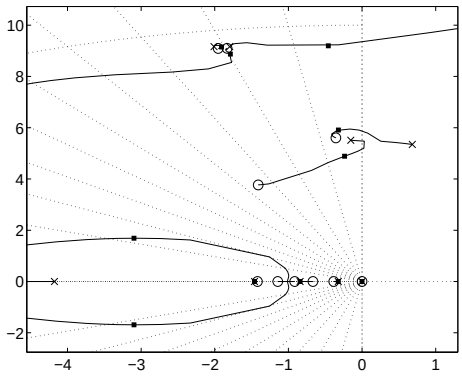

Fig. 16. Root-Locus Design for Delayed Signal

controller in case the Segredo PSS has to go offline. We expect the minimum damping to be higher if T is smaller.

V. Conclusion

In this paper, we show several control design schemes useful for damping of swing modes in a multiple-input, multiple-output system. We discuss the design of decentralized controllers. In addition, we explore the possibilities of stabilizing the system with only s single controller. This implementation requires the use of a remote signal to enhance the control flexibility. Such a study is important in improving reliability in a de-regulated power system, where alternative controller structures can be used for stabilization or as backup to the primary control function.

Acknowledgements

The work of J. Chow, H. Ren, S. Wang is supported in part by an EPRI/DoD CINSI Contract administrated by Carnegie Mellon University.

References

[1] J. F. Hauer, "Robust Damping Control for Large Power Systems," *IEEE Control Systems Magazine,* January 1989, pp. 12-18.

[2] G. E. Boukarim, S. Wang, J. H. Chow, G. N. Taranto and N. Martins, "A Comparison of Classical, Robust, and Decentralized Control Designs for Multiple Power System Stabilizers," to appear in *IEEE Tran. on Power Systems.*

[3] N. Martin and L. T. G. Lima, "Eigenvalue and Frequency Domain Analysis of Small Signal Electromechanical Stability Problem," IEEE Special Publication on Eigenanalysis and Frequency Domain Methods for System Dynamic Performance, 1989, pp. 17-33.

[4] *IEEE Recommended Practice for Excitation System Models for Power System Stability Studies,* IEEE Standard 421.5-1992, 1992.

[5] E. V. Larsen and J. H. Chow, "SVC Control Design Concepts for System Dynamic Performance," IEEE Special Publication on Application of Static var Systems for System Dynamic Performance, 1987, pp. 36-53.

[6] E. V. Larsen, J. J. Sanchez-Gasca, and J. H. Chow, "Concepts for Design of FACTS Controllers to Damp Power Swings," *IEEE Trans. on Power Systems,* vol. 10, 1995, pp. 948-955.

[7] J. H. Chow (editor), Time-Scale Modeling of Dynamic

Networks with Applications to Power Systems, Springer-Verlag, 1982.

[8] S. Wang and J. H. Chow, "Low-Order Controller Design for Model Matching Optimization Using Coprime Factors and Linear matrix Inequalities," to be published in *IEEE Trans. on Automatic Control,* 1999.

[9] S. Wang and J. H. Chow, K. D. Minto, and R. Ravi, "Low-Order Controller Design for Model Matching Optimization Using Coprime Factors and Linear Matrix Inequalities," *Proc. 1999 American Control Conference*, pp. 1871-1875.

[10] M. Chilali and P. Gahinet, "H_∞ Design with Pole Placement Constraints: An LMI Approach," *IEEE Transactions on Automatic Control,* Vol. 41, pp. 358-367, 1996.

[11] P. Gahinet, A. Nemirovskii, A. J. Laub, and M. Chilali, *LMI Control Toolbox: For Use with MATLAB*, The MathWorks, Inc., 1995.

[12] C. Scherer, P. Gahinet, and M. Chilali, "Multiobjective Output-Feedback Control via LMI Optimization," *IEEE Transactions on Automatic Control,* vol. 42, pp. 896-911, 1997.

[13] G. N. Taranto, S. Wang, J. H. Chow, and N. Martins, "Decentralized Design of Power System Damping Controllers using a Linear Matrix Inequality Algrorithm," *Proc. of VI SEPOPE*, 1998.

[14] G. F. Franklin, J. D. Powell, and A. Emami-Naeini, *Feedback Control of Dynamic Systems,* 3rd edition, Addison Wesley, 1995.